

# Tribological Analogy of Cast AA2024/TiB<sub>2</sub> Composites

<sup>1</sup>G. V. R. Kumar and A. Chennakesava Reddy<sup>2</sup>

<sup>1</sup>Research Scholar, Department of Mechanical Engineering, JNTU College of Engineering, Hyderabad, India

<sup>2</sup>Professor, Department of Mechanical Engineering, JNTU College of Engineering, Hyderabad, India  
dr\_acreddy@yahoo.com

**Abstract:** In the current work, the AA2024/TiB<sub>2</sub> metal matrix composites were manufactured at 10% and 30% volume fractions of TiB<sub>2</sub>. The composites were wear tested at different levels of normal load, sliding speed and sliding distances. The microstructure of worn surfaces pertaining to AA2024 alloy/TiB<sub>2</sub> composite reveals the detachment of TiB<sub>2</sub> particles from the matrix.

**Keywords:** Metal matrix composite, AA2024 alloy, titanium boride, wear, sliding distance, normal load, sliding speed.

## 1. INTRODUCTION

Modeling wear is essential for tribological applications of metal matrix composites. Even though mechanical characterization of composite materials has advanced significantly over the past decade, the definition of clear strategies for tribological behavior still remains challenging. It has been established that a proper selection of reinforce and matrix materials may help to widen the scope of metal matrix composites [1-17]. The wear characteristics of the composites depend upon the material morphology [18-22]. The effect of process parameters and the addition of reinforcement on the dry sliding wear of the composites were investigated vastly and explained that incorporation of hard secondary constituent in the matrix significantly improves the wear resistance.

The present work is on the determination of wear characteristics and consequences of cast AA2024/titanium boride composites. The design of experiments was based on Taguchi techniques [23, 24].

**Table 1:** Control parameters and levels

Factor	Symbol	Level-1	Level-2	Level-3
Reinforcement, Vol.%	A	10	20	30
Load, N	B	20	30	40
Speed, m/s	C	2	3	4
Sliding distance, m	D	500	1000	1500

**Table 2:** Orthogonal array (L9) and control parameters

Treat No.	A	B	C	D
1	1	1	1	1
2	1	2	2	2
3	1	3	3	3
4	2	1	2	3
5	2	2	3	1
6	2	3	1	2
7	3	1	3	2
8	3	2	1	3
9	3	3	2	1

## 2. MATERIALS METHODS

The reinforcement material was titanium boride (TiB<sub>2</sub>) nanoparticles of average size 100nm. AA2024 alloy/ TiB<sub>2</sub> composites were fabricated by the stir casting process and low pressure casting technique with argon gas at 3.0 bar. The composite samples were given heat treatment of T6. The heat-treated samples were machined to get cylindrical specimens of dimension 10 mm diameter and 30 mm length for the wear tests. A pin on disc type friction and wear monitor (ASTM G99) was employed to

evaluate the friction and wear behavior of AA2024 alloy/ TiB<sub>2</sub> composites against hardened ground steel (En32) disc. The design of experiments was carried out as per Taguchi techniques. The levels chosen for the controllable process parameters are summarized in Table 1. The orthogonal array L9 was preferred to conduct experiments. An exploration has been carried out to study the effects of sliding speed, contact time, normal pressure, and volume fraction of TiB<sub>2</sub> on the wear characteristics. Scanning electron microscopy analysis was also carried out to find consequence of wear test AA2024/ TiB<sub>2</sub> composite specimens.

Elastic modulus is measure of the stiffness of a material and is a quantity used to characterize materials. Elastic modulus is the same in all orientations for isotropic materials.

The upper-bound equation is given by

$$\frac{E_c}{E_m} = \left( \frac{1-v_v^{2/3}}{1-v_v^{2/3}+v_v} \right) + \frac{1+(\delta-1)v_p^{2/3}}{1+(\delta-1)(v_p^{2/3}-v_p)} \tag{1}$$

The lower-bound equation is given by

$$\frac{E_c}{E_m} = 1 + \frac{v_p-v_v}{\delta/(\delta-1)-(v_p+v_v)^{1/3}} \tag{2}$$

where,  $\delta = E_p/E_m$ .

where,  $v_v$  and  $v_p$  are the volume fractions of voids/porosity and nanoparticles in the composite respectively and  $E_m$  and  $E_p$  is elastic moduli of the matrix and the particle respectively.

The microhardness was measured in terms of Knoop hardness number. The Knoop indenter is a diamond ground to pyramidal form that produces a diamond shaped indentation having approximate ratio between long and short diagonals of 7:1. The depth of indentation is about 1/30 of its length. When measuring the Knoop hardness, only the longest diagonal of the indentation was measured and this was used in the formula mentioned in Eq. (5) with the load used to calculate KHN.

The Knoop hardness number KHN is the ratio of the load applied to the indenter, P (kgf) to the unrecovered projected area:

$$KHN = \frac{P}{CL^2} \tag{3}$$

where,

$P$  = applied load in kgf

$L$  = measured length of long diagonal of indentation in mm

$C = 0.07028$  = Constant of indenter relating projected area of the indentation to the square of the length of the long diagonal.

### 3. RESULTS AND DISCUSSION

The elastic modulus (figure 1a) and knoop hardness (figure 1b) were increased with volume fraction of TiB<sub>2</sub>. This is owing to higher stiffness and hardness of titanium boride nanoparticles than those of AA2024 alloy matrix. At 30% of TiB<sub>2</sub> the elastic stiffness values of AA2024/TiB<sub>2</sub> composites were nearly same as computed by the present model and by Rule of Mixtures (ROM). There is a lot discrepancy at low volume fraction of TiB<sub>2</sub>. This may be due to the ignorance of the effects of porosity and clustering of nanoparticles in the ROM model.

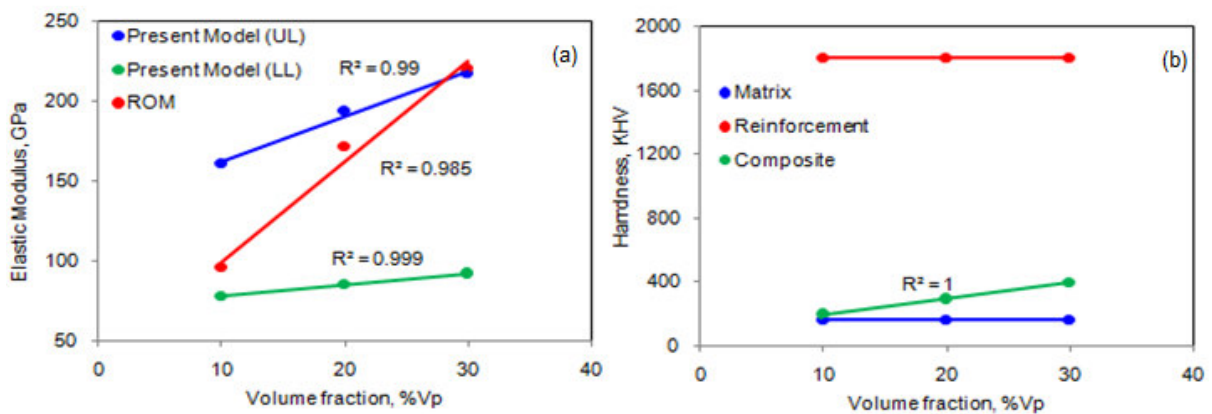


Figure 1: Elastic modulus and hardness of AA2024/TiB<sub>2</sub> composites.

**3.1 Effect of volume fraction, Normal Load, Sliding Speed, Sliding distance on Wear Rate**

For the analysis of variance (ANOVA), all parameters qualify Fisher’s test at 90% confidence level. In Table 3, the percent contribution indicates that the parameter A, assigns 63.41% of variation in the wear rate. The parameter B accords 19.38% of variation in the wear rate. The parameter C contributes 2.02% of variation in the wear rate. The parameter D presents 15.19% of variation in the wear rate.

**Table 3:** ANOVA summary of the effective stress

Source	Sum 1	Sum 2	Sum 3	SS	v	V	F	P
A	23.01	21.34	20.21	1.32	1	1.32	3.10E+13	63.41
B	20.64	21.80	22.12	0.40	1	0.40	9.48E+12	19.38
C	21.68	21.65	21.23	0.042	1	0.042	9.90E+11	2.02
D	21.31	146.44	64.56	0.31	1	0.31	7.43E+12	15.19
e				0.00	4	0.00	1.00E+00	0
T	86.64	211.23	128.12	2.086	8			100

**Note:** SS is the sum of square, v is the degrees of freedom, V is the variance, F is the Fisher’s ratio, P is the percentage of contribution and T is the sum squares due to total variation.

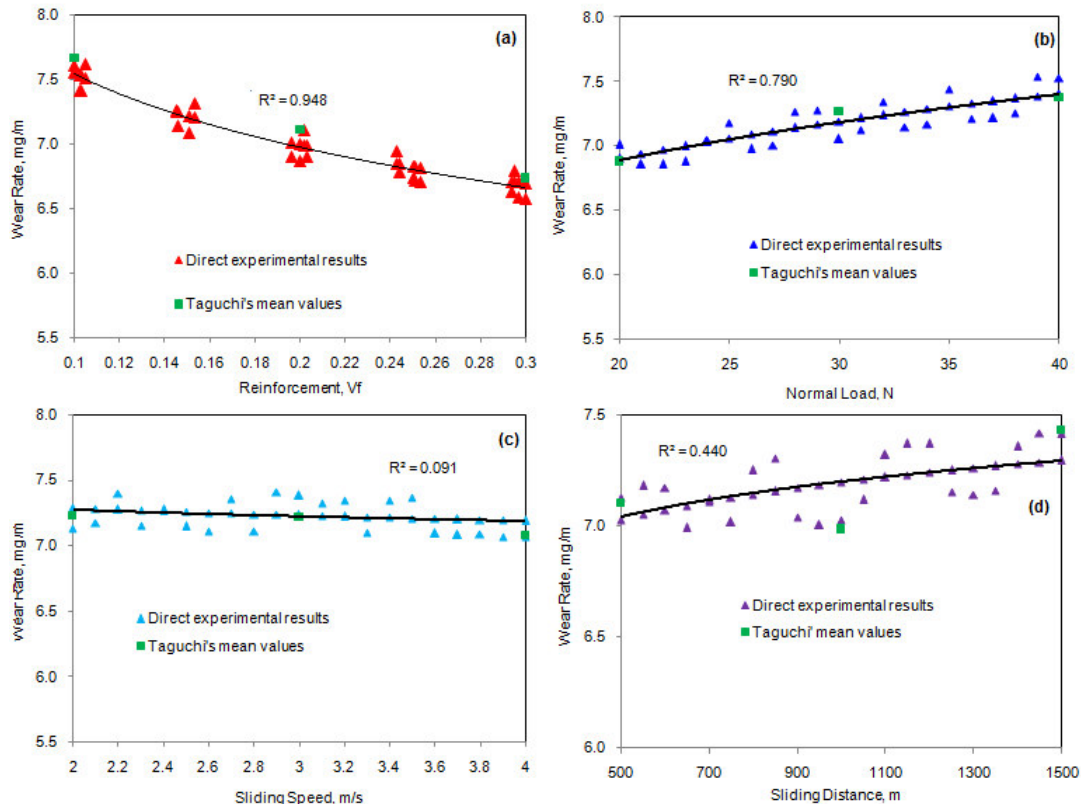


**Figure 2:** Influence of process parameters on wear rate.

The wear test results are shown in figure 2. Owing to high hardness of TiB<sub>2</sub>, the wear rate was decreased with increase in volume fraction of TiB<sub>2</sub> in AA2024 alloy matrix (figure 2a). The wear rate was increased with load regardless of composition of the composites as shown in figure 2b. The wear rate was decreased with increase of sliding speed (figure 2c). The plastic deformation decreases with increasing the sliding speed. From figure 3d it is observed that the wear rate was increased with the sliding distance. The mathematical relations between wear and vol.% of reinforcement, normal load, speed and sliding distance are given by

$$W_{rp} = 5.817 \times v_f^{-0.11} \tag{6}$$

$$W_{rf} = 5.042 \times F^{0.104} \tag{4}$$

$$W_{rn} = 7.37 \times N^{-0.01} \tag{5}$$

$$W_{rd} = 5.769 \times d^{0.032} \tag{6}$$

where,

$W_{rp}$  is the wear rate due to vol.% of reinforcement ( $v_f$ ),  $\text{mm}^3/\text{m}$

$W_{rf}$  is the wear rate due to normal load ( $F$ ),  $\text{mm}^3/\text{m}$

$W_{rn}$  is the wear rate due to speed ( $N$ ),  $\text{mm}^3/\text{m}$

$W_{rd}$  is the wear rate sliding distance ( $d$ ),  $\text{mm}^3/\text{m}$ .

The mathematical expressions were fit into power-law function. In statistics, a power law is a functional relationship between two quantities, where a relative change in one quantity results in a proportional relative change in the other quantity, independent of the initial size of those quantities. One attribute of power laws is their scale invariance. The R-squared values, which are attributable to volume fraction of reinforcement, normal load, sliding speed and sliding distance, are 0.948, 0.790, 0.091 and 0.440, respectively. This trend is similar to the percent contributions of process parameters obtained from Taguchi techniques.

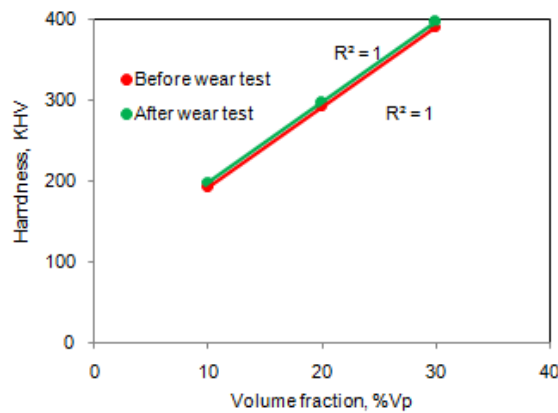


Figure 3: Harness of AA2024/ TiB<sub>2</sub> composites after wear test.

### 3.2 Consequence of Wear in AA2024/ TiB<sub>2</sub> Composites

It is important to settle on the corollary of wear in AA2024/ TiB<sub>2</sub> composites. The change in hardness of the worn specimens is shown in figure 3. It can be seen that the hardness values increase after wear test. The increase in hardness in the worn specimens may be attributed to the work hardening mainly due to influence of volume fraction of TiB<sub>2</sub> and load applied on the wear specimens. The microstructures of worn specimens are revealed in figure 4. When the reinforcement increased from 10% to 30% the scratches and detachment of particles were also increased. The scratches are more in the matrix dominated composites due to its softness; whereas the detachment of nanoparticles is predominant in the reinforcement (i.e., high volume fraction) subjugated composites.

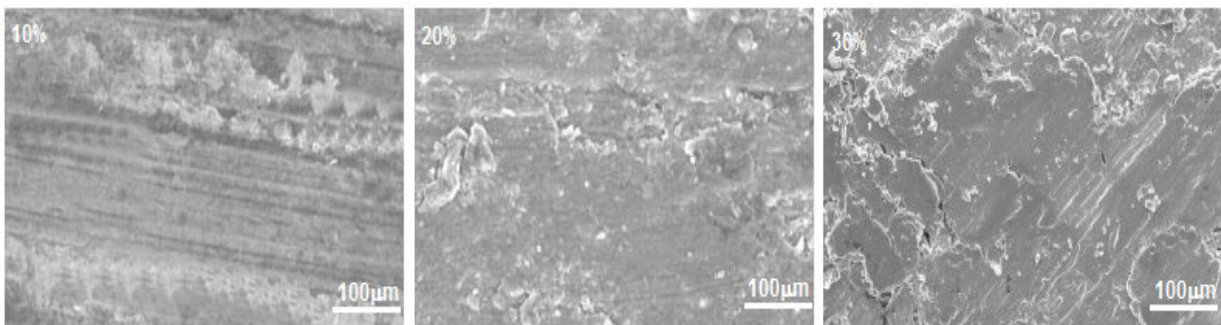


Figure 6: SEM images of worn surfaces of AA2024/ TiB<sub>2</sub> composites: (a) 10 vol.% TiB<sub>2</sub> (b) 20 vol.% TiB<sub>2</sub> and (c) 30 vol.% TiB<sub>2</sub>.

### 3. CONCLUSION

The exploration on the wear behavior of the composites as the function of volume fraction of reinforcement, load, sliding speed and sliding distance using Taguchi's design of experiments was carried out lucratively. The wear loss decreases with increase in volume fraction of TiB<sub>2</sub> in AA2024 alloy matrix; while it increases with load applied on the wear specimens.

### REFERENCES

1. A. C. Reddy, Fracture behavior of brittle matrix and alumina trihydrate particulate composites, *Indian Journal of Engineering & Materials Sciences*, 9, 2002, pp.365-368.
2. A. C. Reddy, S. Sundararajan, Influences of ageing, inclusions and voids on the ductile fracture mechanism of commercial Al-alloys, *Journal of Bulletin of Material Sciences*, 28, 2005, pp. 75-79.
3. A. C. Reddy and Essa Zitoun, Matrix al-alloys for alumina particle reinforced metal matrix composites, *Indian Foundry Journal*, 55, 2009, pp.12-16.
4. A. C. Reddy, Mechanical properties and fracture behavior of 6061/SiCp Metal Matrix Composites Fabricated by Low Pressure Die Casting Process, *Journal of Manufacturing Technology Research*, 1, 2009, pp.273-286.
5. A. C. Reddy and B. Kotiveerachari, Effect of aging condition on structure and the properties of Al-alloy / SiC composite, *International Journal of Engineering and Technology*, 2, 2010, pp.462-465.
6. A. Chennakesava Reddy, Tensile properties and fracture behavior of 6063/SiCP metal matrix composites fabricated by investment casting process, *International Journal of Mechanical Engineering and Materials Sciences*, 3, 2010, pp.73-78.
7. A. C. Reddy and Essa Zitoun, Tensile behavior Of 6063/Al<sub>2</sub>O<sub>3</sub> particulate metal matrix composites fabricated by investment casting process, *International Journal of Applied Engineering Research*, 1, 2010, pp.542-552.
8. A. C. Reddy, Stir Casting Process on Porosity Development and Micromechanical Properties of AA5050/Titanium Oxide Metal Matrix Composites, 5th National Conference on Materials and Manufacturing Processes, Hyderabad, 9-10 June 2006, pp. 144-148.
9. A. C. Reddy, Effect of Porosity Formation during Synthesis of Cast AA4015/Titanium Nitride Particle-Metal Matrix Composites, 5th National Conference on Materials and Manufacturing Processes, Hyderabad, 9-10 June 2006, pp. 139-143.
10. A. C. Reddy, Role of Porosity and Clustering on Performance of AA1100/Boron Carbide Particle-Reinforced Metal Matrix Composites, 6th International Conference on Composite Materials and Characterization, Hyderabad, 8-9 June 2007, pp. 122-127.
11. A. Chennakesava Reddy, Effect of Clustering Induced Porosity on Micromechanical Properties of AA6061/Titanium Oxide Particulate Metal matrix Composites, 6th International Conference on Composite Materials and Characterization, Hyderabad, 8-9 June 2007, pp. 149-154.
12. B. Kotiveera Chari, A. C. Reddy, Bottom-Up Pouring and its Effect on Porosity and Clustering in Casting of AA1100/Silicon Nitride Particle-Reinforced Metal Matrix Composites, 6th National Conference on Materials and Manufacturing Processes, Hyderabad, 8-9 August 2008, pp. 110-114.
13. Essa Zitoun, A. Chennakesava Reddy, Microstructure-Property Relationship of AA3003/Boron Nitride Particle-Reinforced Metal Matrix Composites Cast by Bottom-Up Pouring, 6th National Conference on Materials and Manufacturing Processes, Hyderabad, 8-9 August 2008, pp. 115-119.
14. S. Pitchi Reddy, A. C. Reddy, Effect of Needle-like Brittle Intermetallic Phases on Fracture Behavior of Bottom-up Poured AA5050/Titanium Carbide Particle-Reinforced Metal Matrix Composites, 6th National Conference on Materials and Manufacturing Processes, Hyderabad, 8-9 August 2008, pp. 127-132.
15. S. Pitchi Reddy, A. C. Reddy, Synthesis and Characterization of Zirconium Carbide Nanoparticles Reinforced AA2024 Alloy Matrix Composites Cast by Bottom-Up Pouring, 7th International Conference on Composite Materials and Characterization, Bangalore, 11-12 December 2009, pp. 211-215.
16. Essa Zitoun, A. C. Reddy, Analysis of Micromechanical Behavior of AA3003 Alloy - Graphite Metal Matrix Composites Cast by Bottom-Up Pouring with Regard to Agglomeration and Porosity, 7th International Conference on Composite Materials and Characterization, Bangalore, 11-12 December 2009, pp. 216-220.
17. P. Rami Reddy, A. C.a Reddy, Processing of AA4015-Zirconium Oxide Particulate Metal Matrix Composites by Stir Casting Technology, 7th International Conference on Composite Materials and Characterization, Bangalore, 11-12 December 2009, pp. 221-224.
18. A. C. Reddy, S. Madahava Reddy, Evaluation of dry sliding wear characteristics and consequences of cast Al-Si-Mg-Fe alloys, *ICFAI Journal of Mechanical Engineering*, 3, 2010, pp.1-13.
19. A. C. Reddy, M. Vidya Sagar, Two-dimensional theoretical modeling of anisotropic wear in carbon/epoxy FRP composites: comparison with experimental data, *International Journal of Theoretical and Applied Mechanics*, 6, 2010, pp. 47-57.
20. Sudarshan and M. Surappa, Dry sliding wear of fly ash particle reinforced A356 Al composites, *Wear*, vol. 265, no. 3-4, pp. 349-360, 2008.
21. A. C. Reddy, Wear and Mechanical Behavior of Bottom-Up Poured AA4015/Graphite Particle-Reinforced Metal Matrix Composites, 6th National Conference on Materials and Manufacturing Processes, Hyderabad, 8-9 August 2008, pp. 120-126.
22. A. C. Reddy, Sliding Wear and Micromechanical Behavior of AA1100/Titanium Oxide Metal Matrix Composites Cast by Bottom-Up Pouring, 7th International Conference on Composite Materials and Characterization, Bangalore, 11-12 December 2009, pp. 205-210.
23. A. C. Reddy, V.M. Shamraj, Reduction of cracks in the cylinder liners choosing right process variables by Taguchi method, *Foundry Magazine*, 10, 1998, pp. 47-50.
24. A. C. Reddy, V.S.R. Murti, S. Sundararajan, Control factor design of investment shell mould from coal flyash by Taguchi method, *Indian Foundry Journal*, 45, 1999, pp. 93-98.